Journal Pre-proof

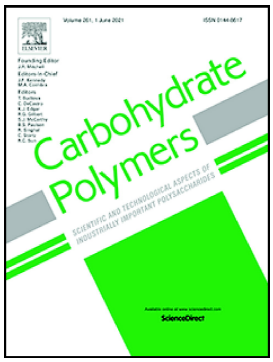

Tailoring nanohole sizes through the deacetylation process in chitosan powders obtained from squid pens

Eliana Lucanera, Sebastián Anbinder, Carlos Macchi, Alberto Somoza

PII: S0144-8617(22)00931-6

DOI: https://doi.org/10.1016/j.carbpol.2022.120026

Reference: CARP 120026

To appear in: *Carbohydrate Polymers*

Received date: 5 May 2022

Revised date: 10 August 2022

Accepted date: 22 August 2022

Please cite this article as: E. Lucanera, S. Anbinder, C. Macchi, et al., Tailoring nanohole sizes through the deacetylation process in chitosan powders obtained from squid pens, *Carbohydrate Polymers* (2022), https://doi.org/10.1016/j.carbpol.2022.120026

Tailoring nanohole sizes through the deacetylation process in chitosan powders obtained from squid pens

Eliana Lucanera, Sebastián Anbinder*, Carlos Macchi, Alberto Somoza

Instituto de Física de Materiales Tandil - IFIMAT (UNCPBA) and CIFICEN (UNCPBA-CICPBA-CONICET), Pinto 399, (B7000GHG) Tandil, Argentina

*Corresponding author: E-mail address: anbinder@exa.unicen.edu.ar (S. Anbinder)

Abstract

An experimental study on the evolution of the physicochemical, thermal and nanostructural properties of chitosan samples obtained from squid pens as the deacetylation treatment proceeds is presented. To this aim, potentiometric titration, capillary viscosimetry, infrared spectroscopy, differential scanning calorimetry and positron annihilation lifetime spectroscopy were used. The results obtained are discussed in terms of the influence of the deacetylation time on the deacetylation degree, average molecular weight, thermal parameters and average free nanohole size of the different samples. A way of preparing chitosan matrices with tailored nanostructural characteristics for specific applications through the deacetylation process is explored.

Keywords: β-chitin; Deacetylation process; Chitosan; Nanostructural properties

1. Introduction

Chitin is a homopolymer composed of β-(1→4)-linked N-acetyl-D-glucosamine (GlcNAc) commonly found in animals, particularly in crustaceans and insects, where it is an essential constituent of the exoskeleton, mollusks, and in certain fungi where it is the principal fibrillar polymer in the cell wall (Roberts, 1992). When this biopolymer is isolated from crab and shrimp shells, it has an α-crystallographic structure in which the main chains present an anti-parallel arrangement with a strong intermolecular hydrogen bonding. In squid pens, a different crystalline polymorph, known as β-chitin, is present. This crystallographic structure is characterized by weaker intermolecular forces due to the parallel disposition of the polymer chains. Despite being the most abundant polysaccharide after cellulose, chitin is not widely used for industrial applications because it is insoluble in many solvents (Kumari & Rath, 2014). By thermochemical alkaline deacetylation of chitin, a linear polysaccharide known as chitosan, is produced. The percentage of glucosamine units (GlcN) in the structure of this biopolymer is known as deacetylation degree (DD%), which plays a key role in the chemical, physical and biological properties of chitin and chitosan. In the literature, this polysaccharide is considered as chitosan when the DD% is higher than 50% (Rinaudo, 2006). On the other hand, the European Chitin Society (EUCHIS) consider that chitin and chitosan should be distinguished according to their solubility in 0.1 M acetic acid; specifically, chitosan being soluble in this solution unlike chitin (Weinhold *et al*., 2009).

The free volume theory was developed several years ago as an attempt to explain thermal, mechanical or diffusive properties of polymers as a function of the temperature, specific volume, thermal expansion coefficients, or viscosity (Fox & Flory, 1948) (Ferry, 1980). This concept is used to explain the relationship between the above-mentioned properties and some variables corresponding to polymer structure such as molecular weight, terminal groups contents, among others (Wypych, 2017).

Many of the main potential applications of chitosan (for example, barrier coatings, drug delivery systems or pollutant adsorption systems) are highly dependent on the matrix free volume. In fact, permeation and/or diffusion of solutes (gases, organic molecules, metal atoms, etc.) and their associated kinetics are related to the average free nanohole sizes of the polymer matrix.

Positron Annihilation Lifetime Spectroscopy (PALS) has proven to be an excellent tool to detect changes at the nanoscale in polymers (Jean, 1990). In fact, PALS is the only analytical technique that makes it possible to directly obtain the size and concentration of the free nanohole volumes in porous materials (Jean, Mallon & Shrader, 2003) (Sharma & Pujari, 2017).

To our knowledge, only a scarce number of works focused on the characterization of chitosan matrices using PALS as main experimental technique has been reported. For example, (Lecaros *et al.*, 2016) reported results of a study of the reversibility of thermoresponsive chitosan/butyl glycidyl ether particles. (Sharma *et al.*, 2013) used PALS to follow changes in the nanohole sizes in chitosan-NiO nanocomposites as a function of the NiO nanoparticles content. (Chaudhary, Went, Nakagawa, Buckman & Sullivan, 2010) studied the influence of the water absorption and the cross-linking on the free nanohole volume in chitosan-nanoclay samples. PALS was used by (Ma *et al.*, 2010) to measure the free volume sizes in chitosan active layers of chitosan/polyacrylonitrile composite membranes as a function of the chitosan/polyacrylonitrile ratio. Authors of the present work used the spectroscopy nuclear technique PALS jointly with Fourier Transformed infrared spectroscopy (FT-IR), UV-vis and Differential Scanning Calorimetry (DSC) to study the structural changes produced in the matrix of chitosan films as a consequence of the adsorption of different amounts of copper and chromium ions (Anbinder, Macchi, Amalvy & Somoza, 2019). These authors reported results about the influence of the grafting process on the morphological and physicochemical properties of chitosan-graft-poly(*n*-butyl acrylate) co-polymers (Anbinder, Macchi, Amalvy & Somoza, 2016). It is worth mentioning that to our knowledge, there are no reported PALS results regarding the influence of the deacetylation process on the nanostructural properties of chitosan-based systems.

In the present work, a systematic study on the evolution of the physicochemical, thermal and nanostructural properties of chitosan samples obtained from squid pens produced as a function of the deacetylation degree is presented. Towards this aim, potentiometric titration, capillary viscosimetry, FT-IR spectroscopy and DSC analytical techniques commonly used in polymer science, jointly with the non-conventional nuclear

spectroscopic technique PALS were used. To carry out the present work it was assumed that it is possible to prepare chitosan matrices with tailored nanostructural characteristics for specific applications through changes in the deacetylation process.

2. Materials and Methods

2.1. Material and chemicals

Squid pens from *Illex argentinus* were obtained and kindly donated by the company Luis Solimeno and sons AS "Planta Mare". NaOH (Anedra), acetic acid (Cicarelli), sodium acetate (Sigma-Aldrich), HCl (Anedra) and ethanol (Anedra) used in this work were of analytical grade and were used without purification.

Squid pen chitin isolation

Squid pens were washed with tap water to remove tissue residues; then, clean pens were dried and minced.

To deproteinize the raw material, pens powder (particle sizes ≤ 0.5 mm) was treated with a 1M NaOH solution in a 1:25 solid/solution ratio at room temperature (RT) under continuous stirring. To determine the treatment time, UV-vis spectroscopy was used to follow the extracted protein in the alkaline solution through the deproteinization process. Toward this aim, the band at 280 nm specific for the presence of tryptophan residues was considered (Chaussard & Domard, 2004). Beyond 5 h of treatment, there was no significant increment in the 280 nm band intensity. Consequently, we have defined 5 h as the time in which an efficient protein removal with minor effects in other sample properties (*i.e.*, MW, DD%) is achieved. Thereby, the suspension was filtered, the solids were washed with deionized water until neutral pH, then with ethanol, and finally dried at 40 °C. As a result, the obtained chitin was a white powder.

Chitosan preparation

Chitin (CH) was suspended in a 40 wt.% aqueous NaOH solution and heated at 90 °C under a nitrogen purge with stirring for 4, 8, 12, 24 and 48 h. The chitin/solution

ratio was 1:100. After the reaction, the chitosan powder was washed with deionized water until neutral pH, then with ethanol and finally dried at 40 °C. The obtained powder was stored in a desiccator until use.

Table 1 summarizes the nomenclature used to identify the studied samples.

Table 1: Nomenclature of the studied samples

Deacetylation time (h)	0	4	8	12	24	48
Sample name	CH	CS04	CS08	CS12	CS24	CS48

2.2. Potentiometric titration (PT)

The different samples were dispersed in a known excess of acid (HCl, 0.1 M) and titrated with a 0.1 M NaOH solution to obtain a curve with two inflection points (titration curves are presented in Figure S.1). The degree of deacetylation was calculated by:

$$DD = \frac{203.195 \times w(NH_2)}{161.02262+0.42037 \times w(NH_2)} \quad [1]$$

where $w(NH_2)$ is the weight fraction of the amino groups:

$$w(NH_2) = 100 \times \frac{V \times c \times 0.016}{W_{dry}} \quad [2]$$

where V represents the volume of consumed titrant (in millilitres) between the two abrupt changes of pH, W_{dry} the dry weight of chitosan sample (in grams) and c the NaOH molar concentration (Zhang, Zhang, Ding Zhang & Liu, 2011). DD and $w(NH_2)$ are expressed as percentages. Experiments were performed in triplicate.

2.3. Viscometric molecular weight

An Ubbelohde capillary viscometer (ϕ=0.5 mm) was used to perform the viscosity measurements at RT following the technique described by Rinaudo, Milas & Dung,

(1993). The viscometric molecular weight (M_v) was calculated using the following equation:

$$\eta = KM_v^{\,a} \qquad [3]$$

where η is the intrinsic viscosity (in mL/g), K and a are empirical constants that depend on the nature of the solvent and the polymer. In this work, a solvent composed of 0.3 M acetic acid/0.2 M sodium acetate was used. According to Rinaudo *et al*. (1993), M_v was calculated using *K=0.074 mL/g* and *a=0.76*. Experiments were performed in triplicate.

2.4. Fourier transformed infrared spectroscopy

FT-IR spectra were performed in the transmission mode using a FT-IR (Nicolet Magna-IR 55) spectrometer in the wavenumber range of 4000 to 400 cm^{-1}, taking 32 scans per spectra, with a resolution of 4 cm^{-1}. Samples were milled, mixed with KBr and then compressed with an hydraulic press at 1 ton. As a result, disks of 10 mm diameter and a typical thickness of about 100 μm were obtained.

In the present work, to calculate the degree of deacetylation, the absorbance ratio A_{1320}/A_{1420} was calculated using the equation proposed by Brugnerotto *et al*. (2001):

$$A_{1420} = \frac{A_{1320}}{0.3822 + 0.03133\,DA} \qquad [4]$$

where A_{1320} and A_{1420} are the absorbance of the bands at 1320 and 1420 cm^{-1}, respectively; and DA is the degree of acetylation. According to the definition of the degree of deacetylation DD% = 100 - DA, the following equation can be derived:

$$DD(\%) = 100 - \left[31.92\,\frac{A_{1320}}{A_{1420}} - 12.2\right] \qquad [5]$$

To obtain the A_{1420} and A_{1320} values from the FT-IR spectra, linear baselines in the ranges [1460-1400 cm^{-1}] and [1340-1290 cm^{-1}] were used, respectively.

2.5. Differential scanning calorimetry

To obtain DSC thermograms, a TA-Q20 calorimeter was used. Samples of ~10 mg were heated at 10 °C/min from 20 °C to 500 °C with N_2 purge (50 mL/min). For the data treatment, the TA Advantage software (v. 5.0.1) was used.

2.6. Positron annihilation lifetime spectroscopy

i) PALS system set-up

PALS spectra were obtained using a "fast-fast" timing coincidence spectrometer with a time resolution of 360 ps in a collinear geometry. A 10 μCi sealed source of ^{22}NaCl deposited onto two thin Kapton foils (7.5 μm thick) sandwiched between two "identical" samples was used as positron source. The spectra were acquired at RT, and typically 1.5-2 x 10^6 counts per spectrum were collected. The PALS parameters reported in this work for each sample are at least an average of ten measurements at the same experimental conditions.

To obtain PALS samples, powders of CH and CS with different deacetylation times were pressure compressed to prepare pairs of disks of 10 mm diameter and 2 mm thickness.

PALS spectra were satisfactorily decomposed into three discrete lifetime components using the *LT10* software (Giebel & Kansy, 2011).

ii) PALS model

According to the common interpretation for PALS measurements in polymers, spectra are deconvoluted into three discrete lifetime components (Jean, 1990), where the shortest lifetime component τ_1 (0.15 – 0.3 ns) is attributed to positrons annihilated into the bulk and to para-Positronium (p-Ps) annihilations and the intermediate component τ_2 (0.35-0.60 ns) is attributed to positrons annihilated in low electron density regions of the structure. The longest lifetime component τ_3 (1.5-2.2 ns) is ascribed to ortho-

Positronium (o-Ps) decay in the nanoholes forming the free volume; this is, $\tau_3 = \tau_{o\text{-}Ps}$. The parameter $I_3 = I_{o\text{-}Ps}$ is the intensity associated with this long-lifetime component.

A correlation between the $\tau_{o\text{-}Ps}$ and the size of the hole is possible assuming a spherical approximation of holes of radii *R*, as expressed using a simple quantum mechanical model; the Tao-Eldrup model (Eldrup, Lightbody & Sherwood, 1981); (Tao, 1972)

$$\tau_{o-Ps} = 0.5\left[\frac{\Delta R}{R+\Delta R} + \frac{1}{2\pi} sen\left(\frac{2\pi R}{R+\Delta R}\right)\right]^{-1} \qquad [6]$$

where $\tau_{o\text{-}Ps}$ is given in ns and ΔR=1.66 Å is an empirical parameter valid for various molecular materials, such as polymers. The average nanohole free volume (v_h) can then be calculated as:

$$v_h = \frac{4}{3}\pi R^3 \qquad [7]$$

In the present work, we have used the simplest approach to get the fractional free nanohole volume (*FFV*), in which the number of the nanoholes forming the free volume is related to the intensity associated with the o-Ps lifetime (Kobayashi *et al.*, 1989); (Wang, Nakanishi, Jean & Sandreczki , 1990). Under this frame, *FFV* can be assumed to be proportional to the number of nanoholes and the average volume of each nanohole. Then, the following semi-empirical equation can be used:

$$FFV = A \,.\, v_h \,.\, I_{o-Ps} \qquad [8]$$

where v_h (in Å^3) is obtained from Eq. (6) and Eq. (7), $I_{o\text{-}Ps}$ (in %) represent the relative number density of free volumes in the material matrix, and *A*=0.0018 is a scale constant (Nakanishi, Wang & Jean, 1988).

3. Results and discussion

As mentioned in Sec. 2.2., the extracted chitin was a white powder, and the subsequent deacetylation process did not induce a color change.

After deproteinization, the chitin content was about 30 wt.% regarding the original weight of the cleaned and dried pens. The performance of the deacetylation step was around ~70 wt.% with respect to the dried chitin; thus, the chitosan production had an overall yield of around ~21 wt.%, which agrees with the values reported by Kurita *et al.*, (1993).

The evolution of the deacetylation degree as a function of time calculated using PT and FT-IR techniques is presented in Fig. 1 and Table 2. In this figure, the results obtained using both techniques have a similar behavior.

Table 2: Deacetylation degree values measured by potentiometric titration (PT) and FT-IR techniques. In the last column, values of the measured molecular weight of samples are also reported (see experimental details below).

Sample	Deacetylation time (h)	DD (%)		M_v (kDa)
		PT	FT-IR	
CH	0	12 ± 2	6.0 ± 0.2	n/d
CS04	4	66 ± 7	58 ± 1	n/d
CS08	8	69 ± 5	69 ± 2	n/d
CS12	12	78 ± 2	78 ± 2	310 ± 23
CS24	24	89 ± 6	86 ± 2	278 ± 18
CS48	48	98 ± 6	89 ± 2	184 ± 17

*"n/d" means not determined. Reported errors are standard deviation (n=3)

Until 12 hours of alkaline deacetylation treatment, DD% values sharply increase until ~80 %; then, a slight increase in this parameter was found, reaching a final value which varies between ~90 and ~98 %.

It is worth mentioning that the treatment conditions used in the deproteinization step were selected in order to preserve the chitin structure as close as possible to that observed in the squid pens.

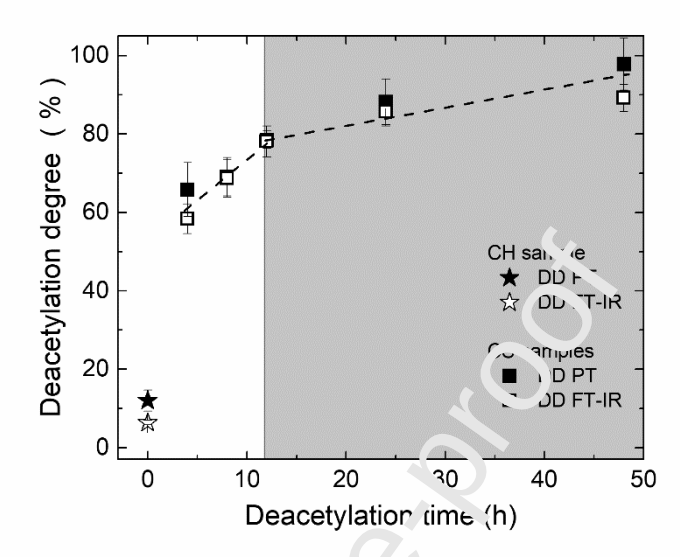

Fig. 1: Deacetylation degree calculated by potentiometric titration and FT-IR as a function of the deacetylation time. Dotted lines are only for an eye guide.

In Fig. 2, the FT-IR spectra of chitin and the different chitosan samples prepared in this work are presented. In Table S.1 presented in Supplementary Information, the usual identification of the main absorption bands of chitosan are listed (Brugnerotto *et al.*, 2001; Kasaai, 2008; Kurita *et al.*, 1993; Mekahlia & Bouzid, 2009; Pawlak & Mucha, 2003). For the FT-IR spectrum corresponding to the obtained CH sample, certain particular bands that correspond to the *β*-chitin are observed; specifically, the single band at 1660 cm^{-1}, which is attributed to the amide I (Kurita *et al.*, 1993; Roberts, 1992) and the shoulder at 3280 cm^{-1} corresponding to the axial deformation of the NH group in the C=O...H–N intermolecular hydrogen bonding (Kurita *et al.*, 1993; Roberts, 1992).

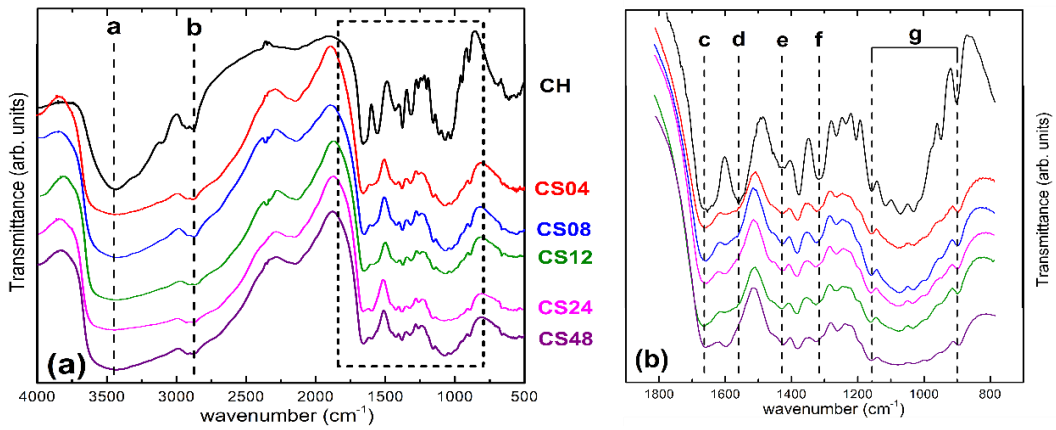

Fig. 2- (a) FT-IR spectra for chitin (CH) and the different deacetylated chitosan (CS) samples. For the sake of clarity, the spectra were arbitrarily shifted in the Y-axis. (b) Zoomed FT-IR spectra in the fingerprint region. The wavenumber assignment of each absorption band labeled from (a) to (g) are given in Table S.1 of Supplementary Information.

Conversely, in Fig. 2 the shoulder at 1627 cm^{-1} typical of *α*-chitin (Focher, Naggi, Torri, Cosani & Terbojevich, 1992; Kurita *et al.*, 1993; Roberts, 1992) is not observed.

As noted in the figure, when the deacetylation treatment proceeds, several changes in different absorption bands occur. Qualitatively, a reduction in the absorbance of the 1660 cm^{-1} amide I band in correspondence with an increase in the absorbance of the 1560 cm^{-1} amide II band is observed. This behavior can be ascribed to changes in the number of acetamide and amine groups, respectively. Moreover, an increase in the absorbance of the 1320 cm^{-1} band assigned to the -NH_2 groups is observed, while the 1420 cm^{-1} reference -CH_2 band remains unchanged. From the absorbance values corresponding to the 1320 and 1420 cm^{-1} bands, the degree of deacetylation defined in Eq. (5) was calculated (see Table S.2).

Furthermore, among the physicochemical parameters of chitosan samples measured in this work, the obtained M_v values are presented in Table 2. As shown in this table, in the range between 12 h and 48 h of the deacetylation treatment, M_v values strongly and systematically decrease from 310 kDa to 167 kDa. In samples with deacetylation treatments shorter than 12 h, specifically, 0 h, 4 h and 8 h; it was not possible to obtain

the viscometric molecular weights values. When the CH, CS04 and CS08 samples were dispersed in the solvent mentioned in Section 2.4, a gel suspension commonly named in the industry as "fish eyes" was obtained. It is known that particles in this kind of colloidal systems are soluble in the outer layers and swollen in the inner layers of the gel formed (Bough, Salter, Wu & Perkins, 1978). Bough *et al*., (1978) reported that this kind of suspension has an extremely high viscosity which does not necessarily imply high molecular weight.

Furthermore, it is possible to obtain indirect information on the changes in chitosan molecular weight by analyzing certain bands in the FT-IR spectrum. Specifically, a diminution in the absorbance of the bands at 1157 cm^{-1} and 890 cm^{-1}, attributed to two different C–O–C vibrations modes on glycosidic linkages (see Table S.1), is indicative of chitosan depolymerization. In Fig. 3, absorbance values obtained for those bands against the deacetylation time are presented. In this figure, a systematic decrease of both absorbances throughout the process can be observed; this behavior is more noticeable during the first 12 h of the deacetylation process. Summarizing, it can be inferred that the chitosan MW is affected by the hydrolysis of the glycosidic bond throughout the alkaline treatment, and the scission of these bonds is more significant in the first stages of the process. This analysis is also supported by the results reported by Tolaimate, Desbrieres, Rhazi & Alagui, (2003) and Tsaih & Chen, (2003).

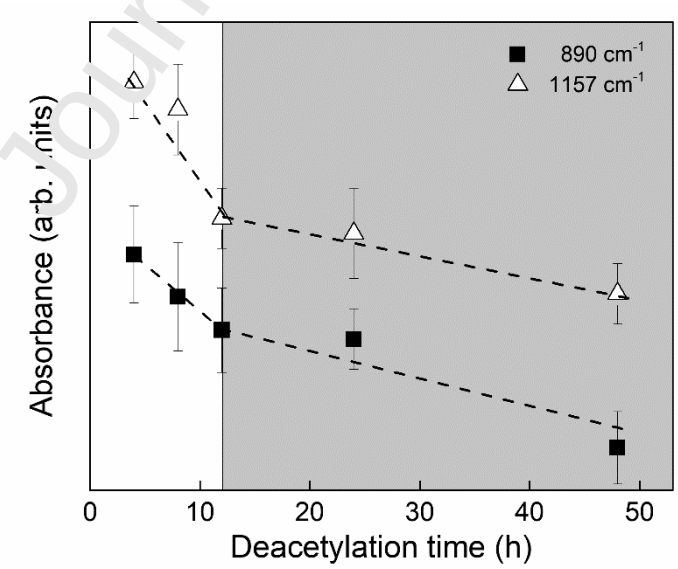

Fig. 3. Peak height of the bands assigned to glycosidic bond as a function of the deacetylation time. Band assignment is presented in Table S.1. Dotted lines are only for eye guide.

In Fig. 4, the DSC thermograms of chitin and chitosan samples treated with different deacetylation times are presented. All the thermograms present a broad endothermic peak in the range of 80°C - 170°C and two exothermic peaks, one around 310°C and the other between 350°C - 450°C. As usual, the endothermic peak is ascribed to the evaporation of bound water in the samples, while the first exothermic peak is attributed to the thermal degradation of the amino (GlcN) groups, and the second one corresponds to the decomposition of the acetamide (GlcNAc) units (Nam, Park, Ihm & Hudson, 2010), (Neto *et al*., 2005).

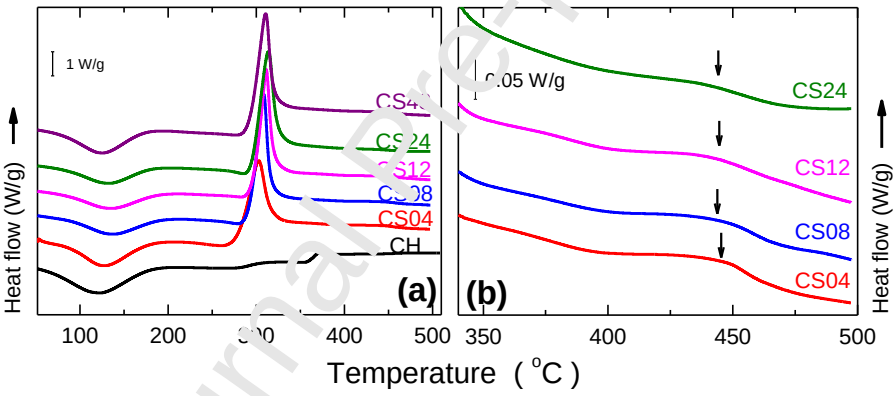

Fig. 4- (a) DSC thermograms of the different deacetyled chitosan samples. The spectra were shifted vertically for the sake of clarity. (b) Zoomed thermograms in the temperature range 350ºC – 500ºC range (see text).

From the *β*-chitin sample DSC thermogram presented in Fig. 4, it can be observed that the exothermic peak at ~310°C is very small when compared with those obtained for the CS samples. This feature owes to the low amount of GlcN residues (~10%, see Table 2) present in the sample.

In Table 3, values of the characteristic parameters of the DSC thermograms, specifically the exotherm temperatures and their corresponding enthalpies, for the CH

and CS samples are presented. In all cases, it can be seen that as the deacetylation reaction proceeds the GlcN exothermic peak area increases while that assigned to GlcNAc decreases. In particular, for the CS48 sample the thermal degradation peak corresponding to the acetamide group in GlcNAc units was non-detectable; this behavior can be attributed to the low content of these functional groups, as reported in Table 2.

Table 3- Thermal parameters obtained from the DSC thermograms presented for the studied samples presented in Fig. 4. The label n/d means non-detectable.

Sample	Deacetylation time (h)	Exotherm (GlcN)		Exotherm (GlcNAc)	
		T_{peak} (°C)	ΔH_{exo} (J/g)	T_{peak} (°C)	ΔH_{exo} (J/g)
CH	0	308	5.3	370	13.9
CS04	4	304	190	443	5.5
CS08	8	308	208	442	4.4
CS12	12	310	215	438	3.6
CS24	24	314	232	434	1.8
CS48	48	310	236	n/d	n/d

In Fig. 5 (a), the thermal degradation enthalpy of the amino groups ΔH_{exo} (GlcN) is presented as a function of the deacetylation time. In this figure, it can be observed that during the first 12 hours of the deacetylation treatment, the ΔH_{exo} (GlcN) for the CS samples linearly increases with the time; for longer deacetylation times the linear increase of the entalphy is significantly slower. It is worth noting that a similar behavior was observed for the parameters reported in Figs. 1 and 3. In Fig.5 (b), the plot

ΔH_{exo} (GlcN) as a function of the deacetylation degree is presented. The observed linear relationship between both parameters is in agreement with that reported by Guinesi & Cavalheiro, (2006). These authors proposed to use the thermal degradation enthalpy of the amino groups as a predictor parameter of the DD% values.

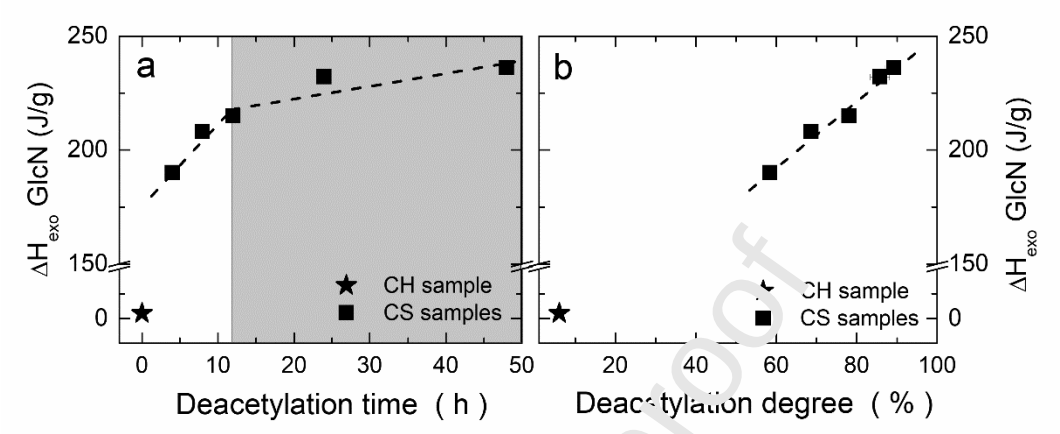

Fig. 5- Thermal degradation enthalpy of amino groups (GlcN) as a function of (a) deacetylation time and (b) deacetylation degree. Dotted lines are only for an eye guide.

In Fig. 6, values of free nanohole volume and the fractional free volume (v_h and *FFV*) as a function of the deacetylation time obtained for the different samples are presented. As shown in the figure, v_h and *FFV* parameters have almost the same behavior. Taking into account Eq. 8 and the results reported in Fig. 6, it can be concluded that the main positron parameter that reveals the nanostructural changes of the CS samples is v_h. Therefore, from now on, the discussion of positron results will be focused in the evolution of the average nanohole size as a function of the deacetylation time.

For the chitin sample, the average nanohole size obtained was 99 $Å^3$. It deserves to be mentioned that, to our knowledge, there are no reported in the literature v_h values for α- or □-chitin.

In Fig. 6, it can be identified two stages of the evolution of the positron parameters (v_h and FFV) for increasing deacetylation times. The first stage, between 0 and 12 h of treatment, is characterized by a sharp linear decrease of both parameters. In the second

stage, for deacetylation times longer than 12 h, a steady linear increase of v_h and FFV is observed.

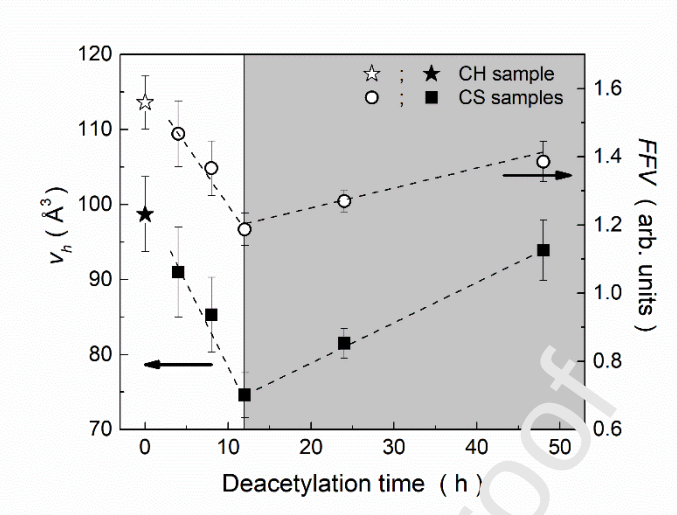

Fig. 6- Free nanohole volumes and fractional free volume as a function of the deacetylation time. Dotted lines are only for an eye guide. Detailed information regarding the values of the different positron parameters is presented in Supplementary Information (see Table S.3).

During the first stage of deacetylation process the v_h values systematically decrease up to about 25 % with respect to CH v_h value. This diminution can be directly associated with that observed in Fig. 1, in which DD% is presented as a function of the deacetylation time. This behavior can be attributed to a systematic replacement of acetamide groups in GlcNAc residues by amine groups in the GlcN residues. The smaller size of the last one allows a better chain arrangement with the consequent diminution of the v_h values (Anbinder *et al.*, 2016).

A drastic change in the nanohole size is observed for deacetylation times longer than 12 h; v_h systematically increase when the treatment proceeds, while DD% slightly increases. Therefore, v_h evolution cannot be only explained in the same terms of those used for the first stage. Under this frame, it must be considered that in addition to changes due to DD% variation with the treatment time, other variables correlated with the free volume should be playing an important role on the nanostructural changes in the chitosan samples.

Yu, Yahsi, McGervey, Jamieson & Simha (1994) used PALS to study the molecular weight-dependence of free volumes in monodisperse polystyrene samples in a wide range of MW. The reported results indicated that the samples with lower average molecular chains have bigger average nanohole sizes. The authors attributed this effect to the contribution of the chain ends to the free volume. From the free volume theory, it is well established that free volumes form close to the chain ends (Ferry, 1980). Based on the Flory-Fox equation, there is a relationship between the free volume and molecular weight. A decrease in the molecular weight is reflected in an increase of the free volume (Ferry, 1980). Therefore, the dominant parameter responsible for the systematic increase of v_h observed for the samples treated between 12 and 48 h is the number of chain ends. On the other hand, for samples treated for times lower than 12 h, the effect of molecular weight changes on the free volume exists, but it is smaller than that of the deacetylation degree.

Summarizing, during the first hours of treatment, when the deacetylation degree sharply increases, the acetamide group hydrolysis is the main process involved in the free volume changes. Once DD% reaches a plateau, depolymerization effects *(i.e.* generation of chain ends free volumes*)* become more important in the average free volume of chitosan samples.

4. Conclusions

For the present work, *β*-chitin isolated from squid pens was deacetylated for increasing times to obtain chitosan powders with different deacetylation degrees. The results obtained indicate that the chitosan nanostructure could be tailored varying the deacetylation time. In this sense, the non-monotonous behavior observed for the average nanohole sizes for increasing treatment times would allow obtaining chitosan matrices with similar nanoholes structure with different deacetylation degrees and molecular weights. This special feature is of utmost importance when preparing chitosan matrices to fulfill specific requirements in their use in, for example, drug delivery or pollutant adsorption systems.

Acknowledgements

The authors acknowledge funding from the Agencia Nacional de Promoción Científica y Tecnológica (Argentina) (PICT 2015-1068 and PICT 2015-1832), Comisión de Investigaciones Científicas de la Provincia de Buenos Aires (Argentina) and Secretaría de Ciencia, Arte y Tecnología SECAT - UNCPBA (Argentina).

References

Anbinder, P., Macchi, C., Amalvy, J., & Somoza, A. (2016). Chitosan-graft-poly(n-butyl acrylate) copolymer: Synthesis and characterization of a natural/synthetic hybrid material. *Carbohydrate Polymers*, *145*, 86–94. https://doi.org/10.1016/j.carbpol.2016.02.072

Anbinder, P. S., Macchi, C., Amalvy, J., & Somoza, A. (2019). A study of the structural changes in a chitosan matrix produced by the adsorption of copper and chromium ions. *Carbohydrate Polymers*, *222*, 114987. https://doi.org/10.1016/j.carbpol.2019.114987

Bough, W. A., Salter, W. L., Wu, A. C. M., & Perkins, B. E. (1978). Influence of manufacturing variables on the characteristics and effectiveness of chitosan products. I. Chemical composition, viscosity, and molecular-weight distribution of chitosan products. *Biotechnology and Bioengineering*, *20*(12), 1931–1943. https://doi.org/10.1002/bit.260201208

Brugnerotto, J., Lizardi, J., Goycoolea, F. M., Argüelles-Monal, W., Desbrières, J., & Rinaudo, M. (2001). An infrared investigation in relation with chitin and chitosan characterization. *Polymer*, *42*(8), 3569–3580. https://doi.org/10.1016/S0032-3861(00)00713-8

Chaudhary, D., Went, M. R., Nakagawa, K., Buckman, S. J., & Sullivan, J. P. (2010). Molecular pore size characterization within chitosan biopolymer using positron annihilation lifetime spectroscopy. *Materials Letters*, *64*(23), 2635–2637. https://doi.org/10.1016/j.matlet.2010.08.045

Chaussard, G., & Domard, A. (2004). New Aspects of the Extraction of Chitin from Squid Pens. *Biomacromolecules*, *5*(2), 559–564. https://doi.org/10.1021/bm034401t

Eldrup, M., Lightbody, D., & Sherwood, J. N. (1981). The temperature dependence of positron lifetimes in solid pivalic acid. *Chemical Physics*, *63*(1), 51–58. https://doi.org/10.1016/0301-0104(81)80307-2

Ferry, J. (1980). *Viscoelastic properties of polymers*. John Wley and Sons.

Focher, B., Naggi, A., Torri, G., Cosani, A., & Terbojevich, M. (1992). Structural differences between chitin polymorphs and their precipitates from solutions—Evidence from CP-MAS 13C-NMR, FT-IR and FT-Raman spectroscopy. *Carbohydrate Polymers*, *17*(2), 97–102. https://doi.org/10.1016/0144-8617(92)90101-U

Fox, T. & Flory, P. (1948). Viscosity—Molecular Weight and Viscosity—Temperature Relationships for Polystyrene and Polyisobutylene. *Journal of the American Chemical Society*, *70*(7), 2384–2395. https://doi.org/10.1021/ja01187a021

Giebel, D., & Kansy, J. (2011). A New Version of LT Program for Positron Lifetime Spectra Analysis. *Materials Science Forum*, *666*, 138–141. https://doi.org/10.4028/www.scientific.net/MSF.666.138

Guinesi, L. S., & Cavalheiro, É. T. G. (2006). The use of DSC curves to determine the acetylation degree of chitin/chitosan samples. *Thermochimica Acta*, *444*(2), 128–133. https://doi.org/10.1016/j.tca.2006.03.003

Jean, Y. C. (1990). Positron annihilation spectroscopy for chemical analysis: A novel probe for microstructural analysis of polymers. *Microchemical Journal*, *42*(1), 72–102. https://doi.org/10.1016/0026-265X(90)90027-3

Jean, Y. C., Mallon, P., & Schrader, D. (2003). *Principles And Applications Of Positron And Positronium Chemistry*. World Scientific.

Kasaai, M. R. (2008). A review of several reported procedures to determine the degree of N-acetylation for chitin and chitosan using infrared spectroscopy. *Carbohydrate Polymers*, *71*(4), 497–508. https://doi.org/10.1016/j.carbpol.2007.07.009

Kobayashi, Y., Zheng, W., Meyer, E. F., McGervey, J. D., Jamieson, A. M., & Simha, R. (1989). Free volume and physical aging of poly(vinyl acetate) studied by positron annihilation. *Macromolecules*, *22*(5), 2302–2306. https://doi.org/10.1021/ma00195a052

Kumari, S., & Rath, P. K. (2014). Extraction and Characterization of Chitin and Chitosan from (Labeo rohit) Fish Scales. *Procedia Materials Science*, *6*, 482–489. https://doi.org/10.1016/j.mspro.2014.07.062

Kurita, K., Tomita, K., Tada, T., Ishii, S., Nishimura, S.-I., & Shimoda, K. (1993). Squid chitin as a potential alternative chitin source: Deacetylation behavior and characteristic properties. *Journal of Polymer Science Part A: Polymer Chemistry*, *31*(2), 485–491. https://doi.org/10.1002/pola.1993.080310220

Lecaros, R. L. G., Syu, Z.-C., Chiao, Y.-H., Wickramasinghe, S. R., Ji, Y.-L., An, Q.-F., Hung, W.-S., Hu, C.-C., Lee, K.-R., & Lai, J.-Y. (2016). Characterization of a Thermoresponsive Chitosan Derivative as a Potential Draw Solute for Forward Osmosis. *Environmental Science & Technology*, *50*(21), 11935–11942. https://doi.org/10.1021/acs.est.6b02102

Ma, J., Zhang, M., Wu, H., Yin, X., Chen, J., & Jiang, Z. (2010). Mussel-inspired fabrication of structurally stable chitosan/polyacrylonitrile composite membrane for pervaporation dehydration. *Journal of Membrane Science*, *1–2*. https://doi.org/10.1016/j.memsci.2009.10.051

Mekahlia, S., & Bouzid, B. (2009). Chitosan-Copper (II) complex as antibacterial agent: Synthesis, characterization and coordinating bond- activity correlation study. *Physics Procedia*, *2*(3), 1045–1053. https://doi.org/10.1016/j.phpro.2009.11.061

Nakanishi, H., Wang, S., & Jean, Y. C. (1988). Microscopic surface tension studied by positron annihilation. In *Positron annihilation studies of fluids* (Sharma, S.C., pp. 292–298). World Scientific.

Nam, Y. S., Park, W. H., Ihm, D., & Hudson, S. M. (2010). Effect of the degree of deacetylation on the thermal decomposition of chitin and chitosan nanofibers. *Carbohydrate Polymers*, *80*(1), 291–295. https://doi.org/10.1016/j.carbpol.2009.11.030

Neto, C., Giacometti, J., Job, A., Ferreira, F., Fonseca, L., & Pereira, M. (2005). Thermal Analysis of Chitosan Based Networks. *Carbohydrate Polymers*, *62*, 97–103.

Pawlak, A., & Mucha, M. (2003). Thermogravimetric and FTIR studies of chitosan blends. *Thermochimica Acta*, *396*(1–2), 153–166. https://doi.org/10.1016/S0040-6031(02)00523-3

Rinaudo, M. (2006). Chitin and chitosan: Properties and applications. *Progress in Polymer Science*, *31*(7), 603–632. https://doi.org/10.1016/j.progpolymsci.2006.06.001

Rinaudo, M., Milas, M., & Dung, P. L. (1993). Characterization of chitosan. Influence of ionic strength and degree of acetylation on chain expansion. *International Journal of Biological Macromolecules*, *15*(5), 281–285. https://doi.org/10.1016/0141-8130(93)90027-J

Roberts, G. A. F. (1992). Structure of Chitin and Chitosan. In G. A. F. Roberts, *Chitin Chemistry* (pp. 1–53). Macmillan Education UK. https://doi.org/10.1007/978-1-349-11545-7_1

Sharma, S. K., Bahadur, J., Patil, P. N., Maheshwari, P., Mukherjee, S., Sudarshan, K., Mazumder, S., & Pujari, P. K. (2013). Revealing the Nano-Level Molecular Packing in Chitosan-NiO Nanocomposite by Using Positron Annihilation Spectroscopy and Small-Angle X-ray Scattering. *ChemPhysChem*, *14*(5), 1055–1062. https://doi.org/10.1002/cphc.201200902

Sharma, S. K., & Pujari, P. K. (2017). Role of free volume characteristics of polymer matrix in bulk physical properties of polymer nanocomposites: A review of positron annihilation lifetime studies. *Progress in Polymer Science*, *75*, 31–47. https://doi.org/10.1016/j.progpolymsci.2017.07.001

Tao, S. J. (1972). Positronium Annihilation in Molecular Substances. *The Journal of Chemical Physics*, *56*(11), 5499–5510. https://doi.org/10.1063/1.1677067

Tolaimate, A., Desbrieres, J., Rhazi, M., & Alagui, A. (2003). Contribution to the preparation of chitins and chitosans with controlled physico-chemical properties. *Polymer*, *44*(26), 7939–7952. https://doi.org/10.1016/j.polymer.2003.10.025

Tsaih, M. L., & Chen, R. H. (2003). The effect of reaction time and temperature during heterogenous alkali deacetylation on degree of deacetylation and molecular weight of resulting chitosan. *Journal of Applied Polymer Science*, *88*(13), 2917–2923. https://doi.org/10.1002/app.11986

Wang, Y. Y., Nakanishi, H., Jean, Y. C., & Sandreczki, T. C. (1990). Positron annihilation in amine-cured epoxy polymers—Pressure dependence. *Journal of Polymer Science Part B: Polymer Physics*, *28*(9), 1431–1441. https://doi.org/10.1002/polb.1990.090280902

Weinhold, M. X., Sauvageau, J. C. M., Keddig, N., Matzke, M., Tartsch, B., Grunwald, I., Kübel, C., Jastorff, B., & Thöming, J. (2009). Strategy to improve the characterization of chitosan for sustainable biomedical applications: SAR guided multi-dimensional analysis. *Green Chemistry*, *11*(4), 498. https://doi.org/10.1039/b809941c

Wypych, G. (2017). *Handbook of Plasticizers*. Elsevier.

Yu, Z., Yahsi, U., McGervey, J. D., Jamieson, A. M., & Simha, R. (1994). Molecular weight-dependence of free volume in polystyrene studied by positron annihilation measurements. *Journal of Polymer Science Part B: Polymer Physics*, *32*(16), 2637–2644. https://doi.org/10.1002/polb.1994.090321609

Zhang, Y., Zhang, X., Ding, R., Zhang, J., & Liu, J. (2011). Determination of the degree of deacetylation of chitosan by potentiometric titration preceded by enzymatic pretreatment. *Carbohydrate Polymers*, *83*(2), 813–817. https://doi.org/10.1016/j.carbpol.2010.08.058

CRediT Author Statement

E. Lucanera: Formal analysis, Investigation, Writing - Original Draft. **P. S. Anbinder**: Conceptualization, Methodology, Formal analysis, Investigation, Writing - Review & Editing. **C. Macchi**: Writing - Review & Editing, Visualization, Formal analysis. **A. Somoza**: Project administration, Funding acquisition, Supervision.

Declaration of interests

The authors declare that they have no known competing financial interests or personal relationships that could have appeared to influence the work reported in this paper.

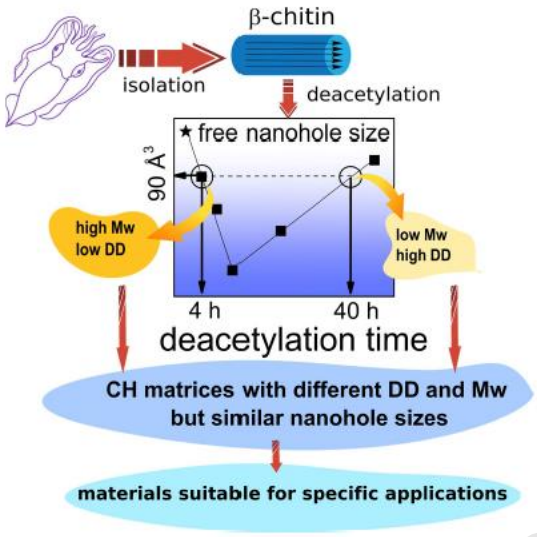

Graphical abstract